HOKKAIDO UNIVERSITY

Title	Involvement of Caveolin-1-mediated transcytosis in the intratumoral accumulation of liposomes
Author(s)	Sakurai, Yu; Kato, Akari; Harashima, Hideyoshi
Citation	Biochemical and biophysical research communications, 525(2), 313-318 https://doi.org/10.1016/j.bbrc.2020.02.086
Issue Date	2020-04-30
Doc URL	https://hdl.handle.net/2115/81106
Rights	©2020. This manuscript version is made available under the CC-BY-NC-ND 4.0 license http://creativecommons.org/licenses/by-nc-nd/4.0/
Rights(URL)	https://creativecommons.org/licenses/by-nc-nd/4.0/
Type	journal article
File Information	WoS_94278_Sakurai.pdf

Hokkaido University Collection of Scholarly and Academic Papers : HUSCAP

Communication

Involvement of Caveolin-1-mediated transcytosis in the intratumoral accumulation of liposomes

Yu Sakurai*, Akari Kato, Hideyoshi Harashima*

Faculty of Pharmaceutical Sciences, Hokkaido University, Sapporo 060-0812, Japan

*Corresponding authors

Correspondence should be addressed to Yu Sakurai (yu-m@pharm.hokudai.ac.jp) or Hideyoshi Harashima (harasima@pharm.hokudai.ac.jp)

Kita-12, Nishi-6, Kita-ku, Sapporo 060-0812, Japan.

Abstract

For achieving efficient cancer treatment, it is important to elucidate the mechanism responsible for the accumulation of nanoparticles in tumor tissue. Recent studies suggest that nanoparticles are not delivered merely through gaps between tumor endothelial cells. We previously reported that the maturation of the vascular structure by the vascular endothelial cell growth factor receptor 2 (VEGFR2) using the previously developed siRNA delivery technology (RGD-MEND) significantly enhanced the accumulation of nanoparticles in vessel-rich types of cancers (renal cell carcinoma). This result was completely inconsistent with the generally accepted theory of the enhanced permeability and retention (EPR) effect. We hypothesized that a caveolin-1 (Cav1)-mediated transcellular route would be involved with the penetration of nanoparticles into tumor vasculature. To reveal the exact mechanism responsible for this enhancement, we observed the delivery of long-circulating liposomes (LPs) after Cav1 was co-suppressed by RGD-MEND with VEGFR2. The enhanced delivery of LPs by siRNA against VEGFR2 (siVEGFR2) was accompanied by the elevated expression of the Cav1 protein. In addition, Cav1 knockdown by siRNA against Cav1 (siCav1) canceled the enhanced delivery of LPs by siVEGFR2. The injection of siCav1 had no effect on the formation of alpha smooth muscle actin or vascular endothelial cell adhesion molecules. These results suggest that a Cav1-induced transcellular route and not a paracellular route, at least partially, contributes to the accumulation of nanoparticles in tumors.

Keywords; EPR effect, cancer, nanoparticle, transcellular, vasculature

Introduction

To enhance the pharmacological effect and circumvent an adverse effects of chemotherapeutics that are used in cancer treatment, a variety of nanoparticles including liposomes (LPs), micelles, polymers have been developed [1,2]. In most cases, the enhanced permeability and retention (EPR) effect is the putative strategy for this accumulation of nanoparticles in the tumor tissue. In the EPR theory, nanoparticles with sizes less than 100 nm with a prolonged circulation time passively accumulate through a malformed vessel structure in the tumor tissue. In tumor tissue, angiogenesis is highly enhanced by angiogenic factors including vascular endothelial cell growth factor-A (VEGF-A) [3,4]. Therefore, the structure of the vasculature in the tumor tissue is clearly altered in comparison with that in normal tissue. Tumor vasculature is characterized by having permeable vessel walls since the tumor vasculature is devoid on lining cells (pericytes), cell adhesion proteins between endothelial cells and a basement membrane [5,6]. Therefore, it is thought that nanoparticles are able to pass through the tumor vasculature, and consequently accumulate in the tumor tissue. The accumulated nanoparticles are not eliminated via the lymphatic system since the lymphatic system in tumor tissue breaks down. Since the EPR effect was first proposed in 1986, a number of different types of nanoparticles have been reported [7]. However, compared to the number of reports on anti-cancer nanoparticles, only a few nanomedicines are used in the clinic [8,9]. In addition, a recent study that conducted a meta-analysis of several clinical studies pointed out that there was no statistical significance in therapeutic effects by nanomedicines in clinic in comparison with free anti-cancer drugs [9]. Some researchers pointed out that the reason for this limitation was differences in the tumor microenvironment between experimental

animals and humans [10,11]. Therefore, to achieve a breakthrough in cancer nanomedicine, the precise mechanism for how nanoparticles are delivered to tumor tissue and a promising strategy for potentiating this delivery through regulating the tumor microenvironment needs to be developed.

To control the tumor microenvironment via the tumor vasculature, we previously developed a liposomal small interfering RNA (siRNA) delivery system equipped with a cyclic RGD peptide (RGD-MEND) [12,13]. The RGD-MEND induced gene silencing in tumor endothelial cells in several cancer models. We revealed that an RGD-MEND encapsulating siRNA against vascular endothelial cell growth factor receptor 2 (VEGFR2) elicited the intratumoral distribution of the subsequently administered LPs with renal cell carcinoma model. Given the fact that VEGFR2 is a dominant protein in cancer angiogenesis, the knockdown of VEGFR2 by the RGD-MEND was accompanied with the maturation of the vasculature, including increased pericyte coverage and increased endothelial cell adhesion. Since LPs are expected to accumulate in tumor tissue through the disrupted vasculature, as described above, this result is inconsistent with the EPR theory. To explain why the accumulation of LPs was substantially improved in spite of the maturation of the vessel structure, we hypothesized that LPs might not pass via the paracellular route but, rather, a transcellular route.

Concerning paclitaxel-conjugated albumin (Abraxane®), this nanocarrier is reported to be transported by transcytosis through the vasculature and that this transport is induced by gp60 [14]. Albumin binds to gp60 on vessels, and is then transcellularly transported to the apical side [15]. The transcytosis occurs through the activation of *Src* and subsequent caveolar-mediated endocytosis [16]. Caveolar-endocytosis is initiated in

cholesterol-rich lipid rafts (calveolae), which are coated with Caveolin-1 (Cav1) [17]. Several studies reported that endothelial Cav1-mediated endocytosis is involved in transcytosis [18,19]. Moreover, this transcytosis was facilitated under conditions of inflammation [20,21]. Since cancer is accompanied by chronic inflammation, this Cav1-mediated endothelial transcytosis would be predicted to be upregulated. Given the above findings and hypotheses, we conclude that Cav1 transcytosis is a possible explanation for the unexpected elevation in the accumulation of the LPs. In this study, using the RGD-MEND, we examined how the accumulation of LPs was significantly elevated by endothelial VEGFR2 knockdown in spite of their mature structures with human renal cell carcinoma model.

Materials and Methods

Materials

1,2-Distearoyl-*sn*-glycerophosphocholine (DSPC) and poly(ethylene glycol) (PEG)-distearoyl-*sn*-glycerophosphoethanolamine (DSPE) were obtained from NOF CORPORATION (Tokyo, Japan). Cholesterol (chol) was obtained from Sigma-Aldrich (St. Louis, MO, USA). YSK05 was synthesized as previously reported [22]. siRNA against siRNA against VEGFR2 was synthesized by Hokkaido System Science (Ishikari, Japan). The sequence of siVEGFR2 was the same as in a previous study [23]; sense: cAAccAGAGAcccucGuuudTsdT, antisense: AAACGAGGGUCUCUGGUUGdTsdT (Upper case is RNA, lower case is 2'-OMethylated RNA, s is thioether instead of phosphorothioated and dT is thymine DNA). siRNA against Cav1 (siCav1) was obtained from ThermoFisher Scientific (Waltham, MA, USA, Assay ID 160016). Other reagents that were used were analytical-grade.

Preparation of tumor-bearing mice

Human renal cell carcinoma OS-RC-2 cells were obtained from the Riken Cell Bank (Tsukuba, Japan). Cells were cultured in RPMI 1640 supplemented with 10% fetal bovine serum and penicillin (100 U/ml), streptomycin (100 μg/ml) at 37 °C and 5% CO_2, respectively. Four-week-old male BALB/cAJcl-nu/nu mice were purchased from CLEA Japan (Shizuoka, Japan). OS-RC-2 cells (1×10^6 cells) in 70 μl PBS were subcutaneously inoculated into the right back. The animals were used when the tumor volume (major axis × minor axis^2/2) reached at 100 mm^3. All experiments were approved by the Hokkaido University Animal Care

Committee.

Preparation of liposomes

DSPC (2,000 nmol), Chol (2,000 nmol) and PEG-DSPE (200 nmol) in $CHCl_3$ were added to a glass tube and DiI was then added to the lipid solution at 0.5 mol% to total lipids. After removing the solvent by a stream of N_2 gas, the lipid thin layer was hydrated by PBS at 60°C. The dispersions were sonicated in a bath-type sonicator for 10 sec. The resulting large LPs were sized by an Extruder with a polycarbonate filter with 400, 200 or 100 nm pores. The final LPs were characterized with a Zetasizer Nano ZS (Malvern Instruments, Malvern, UK).

Preparation of the RGD-MEND

RGD-MEND was prepared as previously described [12,13]. Briefly, YSK05, cholesterol and PEG-DMG were dissolved in ethanol at a molar ratio (70/50, 3 mol%). A solution of siRNA (VEGFR2 or Cav1) solution in 20 mM citrate buffer was then gradually added. The mixture was then subjected to two ultrafiltrations with an Amicon Ultra-14 (Merck-Millipore, Burlington, MA, USA). The obtained lipid nanoparticles were characterized with a Zetasizer Nano ZS. The size of the RGD-MEND particles were typically around 110 nm and the zeta-potential was slightly negative (≈−20 mV). The encapsulation efficiency of siRNA and recovery ratio were measured by a RiboGreen assay, as previously reported [24,25]. The encapsulation efficiency and recovery ratio of the MENDs used in this study were in excess of 90% and 70%, respectively.

Observation of the localization of liposomes by con-focal laser scanning microscopy

The RGD-MEND was systemically administered to mice at a dose of 0.75 or 1.5 mg siRNA/kg three times every other day. DiI-labeled LPs were systemically administered via the tail vein of tumor-bearing mice at a lipid concentration of 200 nmol. Tumor tissue was collected under anesthesia at 24 hours after the injection. After washing the tumor tissue with PBS, slices of the tumor tissue were prepared with a microslicer DTK-1000 (Dosaka-em, Kyoto, Japan) without freezing so as to not affect the localization of the LPs. The slices were stained in 1 μg/mL of Hoechst33342 (Sigma-Aldrich) and 100-times diluted Alexa488 anti-mouse CD31 antibody (Biolegend, clone: MEC13.3). The slices were placed on cover slips (Matsunami, No. 1s), and then observed by an A1R system (Nikon, Tokyo, Japan).

Observation of proteins expression in the tumor tissue.

To evaluate protein expression, tumor tissue was collected 24 hours after the continuous injection of the RGD-MEND. The collected tumor tissues were embedded in optical cutting temperature (O.C.T.) compound (Sakura Finetek, Tokyo, Japan) after fixation in 4% paraformaldehyde. The tissues were cryo-sectioned at thicknesses of 10 μm and then stained with antibodies; for Cav1 Invitrogen, clone:SP43 ; for CD31, ThermoFisher, clone:2H8; for VEcad, first Biolegend, clone:bV13. The antibodies were diluted according to the manufacturer's recommendation. The second antibodies were obtained from ThermoFisher. The slices were covered by cover slips (Matsunami, No. 1s) with a drop of Prolong Gold (ThermoFisher) and then

observed by an A1R system (Nikon, Tokyo, Japan). The analysis for the quantification of images was performed by an Image J software.

Results & Discussion

To confirm our hypothesis that Cav1 is involved in the enhanced accumulation of LPs by VEGFR2 knockdown, the level of expression of Cav1 was followed with changes in the siVEGFR2 dosage (**Figure 1A**). At a dose of 1.5 mg/kg of siVEGFR2, the expression of Cav1 was significantly elevated, but not at a dosage of 0.75 mg/kg (**Figure 1B**). These results were consistent with the findings of a previous study, showing that the injection of siVEGFR2 at a dosage of 0.75 mg/kg did not have a drastic effect on the intratumoral distribution of LPs. In addition, the localization of the increased Cav1 appeared to be specific to the vasculature. We then confirmed the knockdown of Cav1 via a CLSM study (**Figure 2A**). The single knockdown of VEGFR2 resulted in a significant enhancement in the expression of Cav1. It should also be noted that the single siCav1 treatment failed to decrease the levels of Cav1, suggesting that Cav1 on tumor endothelial cells, but not on cancer cells, was induced by VEGFR2 knockdown (**Figure 2B)** The intratumoral distribution of the LPs was then observed (**Figure 2C**). The single knockdown of VEGFR2 substantially improved the intratumoral distribution of the LPs. On the other hand, the single knockdown of Cav1 had no effect on the intratumoral distribution of the particles. However, the knockdown of both VEGFR2 and Cav1 canceled the improvement in the LP distribution caused by the single knockdown of VEGFR2, indicating that Cav1 in the tumor tissue is involved in the intratumoral distribution of LPs, accounting for at least part of the enhancement caused by the VEGFR2 knockdown [26]. Since our previous study revealed that the knockdown by the RGD-MEND was specific to tumor endothelial cells, this indicates that a relationship exists between endothelial Cav1 and the accumulation of LPs in the tumor tissue through the vessel wall

[13].). The combination of siVEGFR2 and siCav1 completely canceled the elevation in Cav1 expression. Finally, to exclude the possibility that the siCav1 treatment disrupted the rigid structure of the tumor vasculature, the levels of alpha smooth muscle actin (αSMA) and vascular endothelial cadherin (VEcad), which are generally regarded as maturation markers, were examined. Their expressions in the vasculature were strongly correlated with the integrity of the vasculature [27,28]. The injection of siVEGFR2 significantly upregulated the expression of αSMA and VEcad, indicating that the treatment induced the maturation of the tumor vasculature (**Figure 3A**). However, the expression of αSMA and VEcad were not altered by the siCav1 single or the siCav1/siVEGFR2 double knockdown, which was confirmed by the quantitative analysis of images (**Figure 3B**). Collectively, the reduced accumulation in the tumor tissue via Cav1 knockdown would not be caused by the enhanced permeability in the tumor vasculature.

It is generally assumed that the maturation of the structure of the tumor vasculature blocks the accumulation of LPs in the tumor tissue via the paracellular route. Our results clearly indicate that the expression of endothelial Cav1 plays a pivotal role in the accumulation of LPs, at least in the case where the accumulation was elevated by the inhibition of VEGF signaling. Moreover, based an examination of the vasculature structure, this extravasation of LPs appeared to occur via the transcellular route and not paracellular route with renal cell carcinoma model. In our previous study, this VEGFR2 knockdown-induced elevation occurred in vessel-rich cancer (hepatocellular carcinoma) but not in vessel-poor cancer (colorectal cancer, breast cancer) [29]. Smith *et al.* reported that tumor type was classified into vessel in stroma (vessel-poor, termed “stroma-vessel type”) and vessel in cancer cells (vessel-rich, termed “tumor-vessel”), and that

only tumor-vessel type cancer was responded to anti-VEGF therapy [30]. Thus, the accumulation elevated by VEGFR2 knockdown might been observed only in a specific type of cancers. On the other hand, it was not clear whether the involvement of Cav1 with the translocation from the vessel lumen to cancer parenchyma. Further study of the relationship between Cav1 expression and the accumulation of nanoparticles in tumor tissue will be needed in order to elucidate the exact mechanism of nanoparticle distribution in tumor tissue.

Recent studies suggest that dynamic molecular biology contributes to the accumulation of nanoparticles. The results of a recent intravital imaging study suggested that nanoparticles were transiently released from the tumor vasculature to the interstitial space of a tumor, functioning as a vent, a process that was referred to as an “eruption” [31]. The eruption randomly occurred at different sites in the tumor tissues. This study also suggested that the vent did not limit the size of nanoparticles, which is contrary to the current thinking regarding the EPR effect. In the EPR effect theory, the adequate size of nanoparticles is severely limited. Since nanoparticles are thought to pass through the intercellular gap and/or the fenestrae, indicative of a transcellular pore, in the tumor vasculature, the optimum size of nanoparticles is considered to be approximately 100 nm [32,33]. In our previous study, VEGFR2 knockdown enhanced the accumulation of LPs even those sizes of 400 nm with renal cell carcinoma model [29]. The elevated permeability of LPs caused by VEGFR2 knockdown can be attributed to eruption-like dynamics. Another study revealed that the delivery of LPs was accompanied by the extravasation of neutrophils [34]. It was reported that neutrophils opened the basement membrane thus allowing LPs to leak from this opening and that net neutrophil

localization was correlated with neutrophil infiltration. Lipopolysaccharide (LPS)/N-acetylgalactose-induced neutrophil infiltration was reported to be significantly attenuated in Cav1 knockout mice [35]. In addition, the deletion of Cav1 suppressed the formation of nuclear factor κB (NFκB) and intracellular cell adhesion molecules-1 (ICAM-1) on liver endothelial cells [36]. Circulating neutrophils recognize endothelial ICAM-1 that is induced by inflammation and initiates infiltration to the inflammatory tissue [17]. Thus, the expression of endothelial Cav1 caused by VEGFR2 might induce the accumulation of LPs. As of this writing, the issue of whether Cav1-mediated accumulation occurs in the untreated tumor endothelium remains unclear. In physiological conditions, oxidized low density lipoprotein (oxLDL) was reported to be internalized via Cav1-mediated endocytosis, and subsequently transported to the apical side by endothelial cells [17]. There are some reports suggesting that LPs sometimes behave like lipoproteins. Since apolipoprotein E (ApoE) in the blood binds to lipid nanoparticles, systemically administered lipid nanoparticles associated with ApoE were internalized via LDL receptors in hepatocytes [37,38]. This lipoprotein-like behavior of LPs can be attributed to Cav1-mediated endocytosis in the tumor tissue. If so, this elevation in accumulation by VEGFR2 knockdown might be limited only to LPs. Therefore, further study will be needed to clarify the contribution of Cav1-mediated delivery in a wide variety of cancer types and nanoparticle types.

Acknowledgements

The authors wish to thank Dr. Milton S Feather for appropriately modifying the manuscript. This study was supported, in part, by Ministry of Health, Labour and Welfare, by Ministry of Education, Culture, Sports,

Science and Technology, by Japan Society for the Promotion of Science KAKENHI (Grant No. 18K18351) , by the Ichiro-Kanehara foundation and by The Mochida Memorial Foundation for Medical and Pharmaceutical Research.

References

[1] Y.S. Youn, Y.H. Bae, Perspectives on the past, present, and future of cancer nanomedicine, Adv Drug Deliv Rev 130 (2018) 3-11. 10.1016/j.addr.2018.05.008.

[2] W. Huang, L. Chen, L. Kang, M. Jin, P. Sun, X. Xin, Z. Gao, Y.H. Bae, Nanomedicine-based combination anticancer therapy between nucleic acids and small-molecular drugs, Adv Drug Deliv Rev 115 (2017) 82-97. 10.1016/j.addr.2017.06.004.

[3] R.S. Apte, D.S. Chen, N. Ferrara, VEGF in Signaling and Disease: Beyond Discovery and Development, Cell 176 (2019) 1248-1264. 10.1016/j.cell.2019.01.021.

[4] M. Simons, E. Gordon, L. Claesson-Welsh, Mechanisms and regulation of endothelial VEGF receptor signalling, Nat Rev Mol Cell Biol 17 (2016) 611-625. 10.1038/nrm.2016.87.

[5] K. Hida, N. Maishi, C. Torii, Y. Hida, Tumor angiogenesis--characteristics of tumor endothelial cells, Int J Clin Oncol 21 (2016) 206-212. 10.1007/s10147-016-0957-1.

[6] K. Hida, N. Maishi, Y. Sakurai, Y. Hida, H. Harashima, Heterogeneity of tumor endothelial cells and drug delivery, Adv Drug Deliv Rev 99 (2016) 140-147. 10.1016/j.addr.2015.11.008.

[7] Y. Matsumura, H. Maeda, A new concept for macromolecular therapeutics in cancer chemotherapy:

mechanism of tumoritropic accumulation of proteins and the antitumor agent smancs, Cancer Res 46 (1986) 6387-6392.

[8] J.W. Nichols, Y.H. Bae, EPR: Evidence and fallacy, J Control Release 190 (2014) 451-464. 10.1016/j.jconrel.2014.03.057.

[9] F. Danhier, To exploit the tumor microenvironment: Since the EPR effect fails in the clinic, what is the future of nanomedicine?, J Control Release 244 (2016) 108-121. 10.1016/j.jconrel.2016.11.015.

[10] U. Prabhakar, H. Maeda, R.K. Jain, E.M. Sevick-Muraca, W. Zamboni, O.C. Farokhzad, S.T. Barry, A. Gabizon, P. Grodzinski, D.C. Blakey, Challenges and key considerations of the enhanced permeability and retention effect for nanomedicine drug delivery in oncology, Cancer Res 73 (2013) 2412-2417. 10.1158/0008-5472.CAN-12-4561.

[11] J.I. Hare, T. Lammers, M.B. Ashford, S. Puri, G. Storm, S.T. Barry, Challenges and strategies in anti-cancer nanomedicine development: An industry perspective, Adv Drug Deliv Rev 108 (2017) 25-38. 10.1016/j.addr.2016.04.025.

[12] T. Hada, Y. Sakurai, H. Harashima, Optimization of a siRNA Carrier Modified with a pH-Sensitive Cationic Lipid and a Cyclic RGD Peptide for Efficiently Targeting Tumor Endothelial Cells, Pharmaceutics 7 (2015) 320-333. 10.3390/pharmaceutics7030320.

[13] Y. Sakurai, H. Hatakeyama, Y. Sato, M. Hyodo, H. Akita, N. Ohga, K. Hida, H. Harashima, RNAi-mediated gene knockdown and anti-angiogenic therapy of RCCs using a cyclic RGD-modified liposomal-siRNA system, J Control Release 173 (2014) 110-118. 10.1016/j.jconrel.2013.10.003.

[14] D. Sleep, Albumin and its application in drug delivery, Expert Opin Drug Deliv 12 (2015) 793-812. 10.1517/17425247.2015.993313.

[15] S.M. Vogel, R.D. Minshall, M. Pilipovic, C. Tiruppathi, A.B. Malik, Albumin uptake and transcytosis in endothelial cells in vivo induced by albumin-binding protein, Am J Physiol Lung Cell Mol Physiol 281 (2001) L1512-1522. 10.1152/ajplung.2001.281.6.L1512.

[16] A.N. Shajahan, C. Tiruppathi, A.V. Smrcka, A.B. Malik, R.D. Minshall, Gbetagamma activation of Src induces caveolae-mediated endocytosis in endothelial cells, J Biol Chem 279 (2004) 48055-48062. 10.1074/jbc.M405837200.

[17] P. Alcaide, S. Auerbach, F.W. Luscinskas, Neutrophil recruitment under shear flow: it's all about endothelial cell rings and gaps, Microcirculation 16 (2009) 43-57. 10.1080/10739680802273892.

[18] C. Tiruppathi, T. Naqvi, Y. Wu, S.M. Vogel, R.D. Minshall, A.B. Malik, Albumin mediates the transcytosis of myeloperoxidase by means of caveolae in endothelial cells, Proc Natl Acad Sci U S A 101 (2004) 7699-7704. 10.1073/pnas.0401712101.

[19] S.A. Predescu, D.N. Predescu, A.B. Malik, Molecular determinants of endothelial transcytosis and their role in endothelial permeability, Am J Physiol Lung Cell Mol Physiol 293 (2007) L823-842. 10.1152/ajplung.00436.2006.

[20] M. Karin, F.R. Greten, NF-kappaB: linking inflammation and immunity to cancer development and progression, Nat Rev Immunol 5 (2005) 749-759. 10.1038/nri1703.

[21] G.C. Hu, S.M. Vogel, D.J. Visintine, A.B. Malik, R.D. Minshall, Activation of endothelial cell ICAM-1

stimulates caveolae-mediated transcytosis, Faseb J 20 (2006) A1166-A1167.

[22] Y. Sato, H. Hatakeyama, Y. Sakurai, M. Hyodo, H. Akita, H. Harashima, A pH-sensitive cationic lipid facilitates the delivery of liposomal siRNA and gene silencing activity in vitro and in vivo, J Control Release 163 (2012) 267-276. 10.1016/j.jconrel.2012.09.009.

[23] J.E. Dahlman, C. Barnes, O. Khan, A. Thiriot, S. Jhunjunwala, T.E. Shaw, Y. Xing, H.B. Sager, G. Sahay, L. Speciner, A. Bader, R.L. Bogorad, H. Yin, T. Racie, Y. Dong, S. Jiang, D. Seedorf, A. Dave, K.S. Sandu, M.J. Webber, T. Novobrantseva, V.M. Ruda, A.K.R. Lytton-Jean, C.G. Levins, B. Kalish, D.K. Mudge, M. Perez, L. Abezgauz, P. Dutta, L. Smith, K. Charisse, M.W. Kieran, K. Fitzgerald, M. Nahrendorf, D. Danino, R.M. Tuder, U.H. von Andrian, A. Akinc, A. Schroeder, D. Panigrahy, V. Kotelianski, R. Langer, D.G. Anderson, In vivo endothelial siRNA delivery using polymeric nanoparticles with low molecular weight, Nat Nanotechnol 9 (2014) 648-655. 10.1038/nnano.2014.84.

[24] Y. Sakurai, T. Hada, A. Kato, Y. Hagino, W. Mizumura, H. Harashima, Effective Therapy Using a Liposomal siRNA that Targets the Tumor Vasculature in a Model Murine Breast Cancer with Lung Metastasis, Mol Ther Oncolytics 11 (2018) 102-108. 10.1016/j.omto.2018.10.004.

[25] Y. Sakurai, H. Hatakeyama, H. Akita, H. Harashima, Improvement of doxorubicin efficacy using liposomal anti-polo-like kinase 1 siRNA in human renal cell carcinomas, Mol Pharm 11 (2014) 2713-2719. 10.1021/mp500245z.

[26] Y. Sakurai, T. Hada, S. Yamamoto, A. Kato, W. Mizumura, H. Harashima, Remodeling of the Extracellular Matrix by Endothelial Cell-Targeting siRNA Improves the EPR-Based Delivery of 100 nm Particles, Mol Ther 24

(2016) 2090-2099. 10.1038/mt.2016.178.

[27] M. Giannotta, M. Trani, E. Dejana, VE-cadherin and endothelial adherens junctions: active guardians of vascular integrity, Dev Cell 26 (2013) 441-454. 10.1016/j.devcel.2013.08.020.

[28] B. Hinz, V. Dugina, C. Ballestrem, B. Wehrle-Haller, C. Chaponnier, Alpha-smooth muscle actin is crucial for focal adhesion maturation in myofibroblasts, Mol Biol Cell 14 (2003) 2508-2519. 10.1091/mbc.e02-11-0729.

[29] S. Yamamoto, A. Kato, Y. Sakurai, T. Hada, H. Harashima, Modality of tumor endothelial VEGFR2 silencing-mediated improvement in intratumoral distribution of lipid nanoparticles, J Control Release 251 (2017) 1-10. 10.1016/j.jconrel.2017.02.010.

[30] N.R. Smith, D. Baker, M. Farren, A. Pommier, R. Swann, X. Wang, S. Mistry, K. McDaid, J. Kendrew, C. Womack, S.R. Wedge, S.T. Barry, Tumor stromal architecture can define the intrinsic tumor response to VEGF-targeted therapy, Clin Cancer Res 19 (2013) 6943-6956. 10.1158/1078-0432.CCR-13-1637.

[31] Y. Matsumoto, J.W. Nichols, K. Toh, T. Nomoto, H. Cabral, Y. Miura, R.J. Christie, N. Yamada, T. Ogura, M.R. Kano, Y. Matsumura, N. Nishiyama, T. Yamasoba, Y.H. Bae, K. Kataoka, Vascular bursts enhance permeability of tumour blood vessels and improve nanoparticle delivery, Nat Nanotechnol 11 (2016) 533-538. 10.1038/nnano.2015.342.

[32] S.K. Golombek, J.N. May, B. Theek, L. Appold, N. Drude, F. Kiessling, T. Lammers, Tumor targeting via EPR: Strategies to enhance patient responses, Adv Drug Deliv Rev 130 (2018) 17-38. 10.1016/j.addr.2018.07.007.

[33] Y. Nakamura, A. Mochida, P.L. Choyke, H. Kobayashi, Nanodrug Delivery: Is the Enhanced Permeability and Retention Effect Sufficient for Curing Cancer?, Bioconjug Chem 27 (2016) 2225-2238.

10.1021/acs.bioconjchem.6b00437.

[34] V.A. Naumenko, K.Y. Vlasova, A.S. Garanina, P.A. Melnikov, D.M. Potashnikova, D.A. Vishnevskiy, S.S. Vodopyanov, V.P. Chekhonin, M.A. Abakumov, A.G. Majouga, Extravasating Neutrophils Open Vascular Barrier and Improve Liposomes Delivery to Tumors, ACS Nano 13 (2019) 12599-12612. 10.1021/acsnano.9b03848.

[35] T.H. Tsai, K. Tam, S.F. Chen, J.Y. Liou, Y.C. Tsai, Y.M. Lee, T.Y. Huang, S.K. Shyue, Deletion of caveolin-1 attenuates LPS/GalN-induced acute liver injury in mice, J Cell Mol Med 22 (2018) 5573-5582. 10.1111/jcmm.13831.

[36] S. Garrean, X.P. Gao, V. Brovkovych, J. Shimizu, Y.Y. Zhao, S.M. Vogel, A.B. Malik, Caveolin-1 regulates NF-kappaB activation and lung inflammatory response to sepsis induced by lipopolysaccharide, J Immunol 177 (2006) 4853-4860. 10.4049/jimmunol.177.7.4853.

[37] C.L. Bisgaier, M.V. Siebenkas, K.J. Williams, Effects of apolipoproteins A-IV and A-I on the uptake of phospholipid liposomes by hepatocytes, J Biol Chem 264 (1989) 862-866.

[38] A. Akinc, W. Querbes, S. De, J. Qin, M. Frank-Kamenetsky, K.N. Jayaprakash, M. Jayaraman, K.G. Rajeev, W.L. Cantley, J.R. Dorkin, J.S. Butler, L. Qin, T. Racie, A. Sprague, E. Fava, A. Zeigerer, M.J. Hope, M. Zerial, D.W. Sah, K. Fitzgerald, M.A. Tracy, M. Manoharan, V. Koteliansky, A. Fougerolles, M.A. Maier, Targeted delivery of RNAi therapeutics with endogenous and exogenous ligand-based mechanisms, Mol Ther 18 (2010) 1357-1364. 10.1038/mt.2010.85.

Figure/Table Legends

Figure 1 The expression of Cav1 is elevated by VEGFR2 knockdown. A) The expression of Cav1 was observed by CLSM after the injection of the RGD-MEND at a dose of 0.75 or 1.5 mg siRNA/kg. Green and red dots indicate CD31 and Cav1, respectively. Scale bars: 50 μm. B) The Cav1 on the tumor vasculature was quatified. Data represents mean ± standard deviation (SD). **: $P<0.01$ (ANOVA followed by SNK test, n=3~6)

Figure 2 Knockdown of Cav1 and cancelation of the improvement in tumor accumulation by Cav1 knockdown. A) The expression of Cav1 in the tumor tissue was evaluated. Green and red dots mean vessels and Cav1, respectively. Scale Bars: 50 μm. B) The Cav1 expression was quantified. The green dots colocalized with red dots (i.e. yellow dots) were counted by an Image J software. Data represents mean ± SD. *: $P<0.01$ (ANOVA followed by Bonferroni test, n=3~11). C) The localization of systemically administered LPs was observed. Tumor tissue was collected 24 hours after systemic injection. Tumor samples were sliced by a microslicer and then stained by anti-CD31-Alexa488 antibody. Green and red dots mean vessels and LPs, respectively. Scale bars: 50 μm.

Figure 4 The structure of the tumor vasculature after VEGFR2 and/or Cav1 knockdown. The expression of αSMA (upper figures) and VEcad (lower figures). Green pixels mean vessels. Red dots represent αSMA (upper figures) and VEcad (lower figures), respectively. Scale bars: 50 μm. B) The αSMA and VEcad expression was quantified. The green dots colocalized with red dots (i.e. yellow dots) were counted by an Image J software. Data represents mean ± SD. *: $P<0.01$ (ANOVA followed by Bonferroni

test, n=3~11).

Figures/Tables

Figure 1

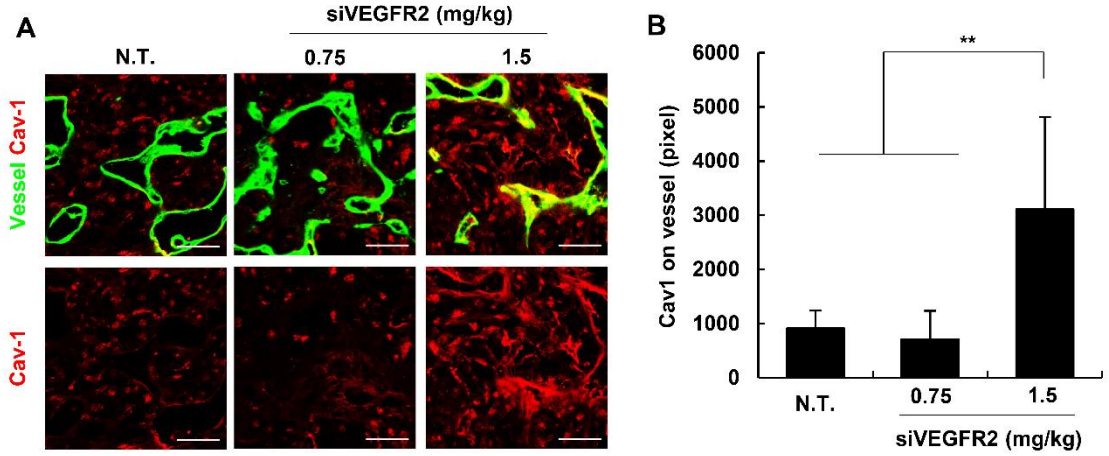

Figure 2

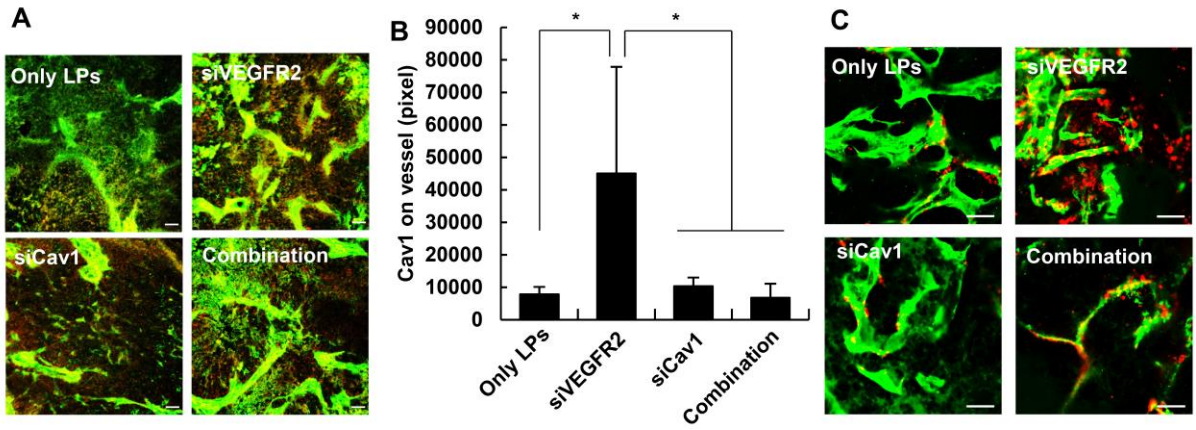

Figure 3

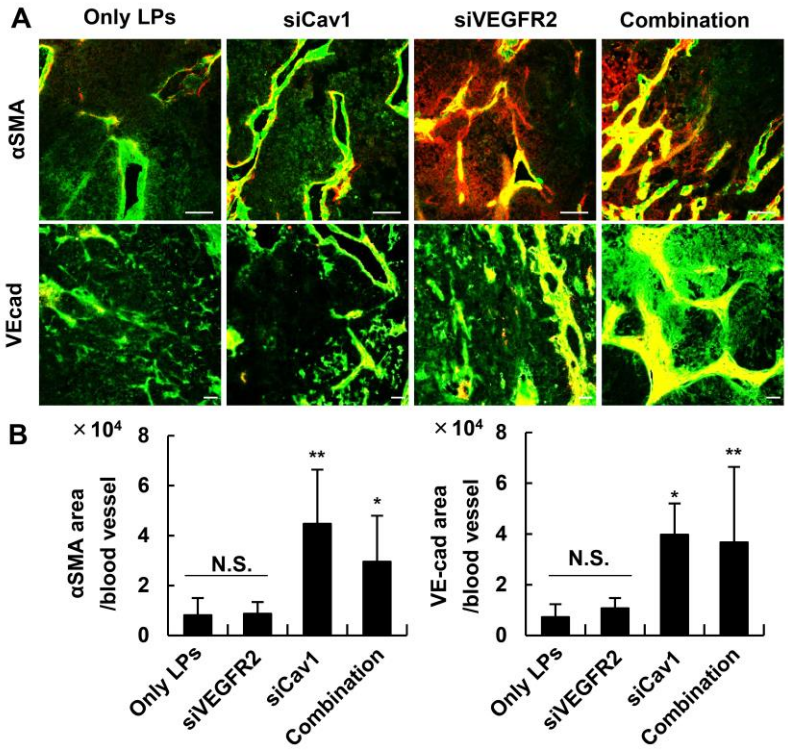
A
Only LPs
siCav1
siVEGFR2
Combination
αSMA
VEcad
B
× 10^4
αSMA area /blood vessel
N.S.
**
*
Only LPs
siVEGFR2
siCav1
Combination
VE-cad area /blood vessel
N.S.
*
**
Only LPs
siVEGFR2
siCav1
Combination